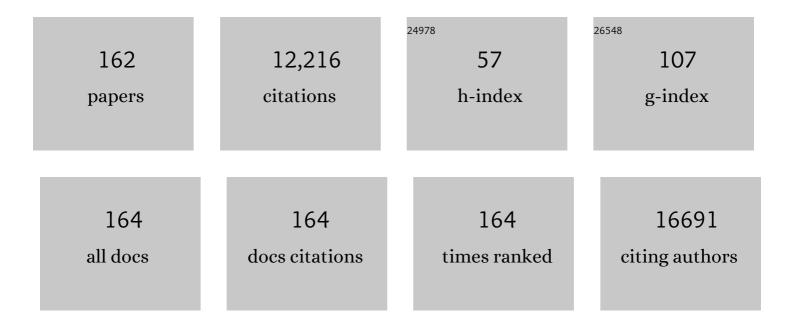
List of Publications by Year in descending order

Source: https://exaly.com/author-pdf/3375068/publications.pdf Version: 2024-02-01



#	Article	IF	CITATIONS
1	Phosphatidic acid modulates MPK3- and MPK6-mediated hypoxia signaling in Arabidopsis. Plant Cell, 2022, 34, 889-909.	3.1	31
2	Ceramides regulate defense response by binding to RbohD in <i>Arabidopsis</i> . Plant Journal, 2022, 109, 1427-1440.	2.8	9
3	The Two Classes of Ceramide Synthases Play Different Roles in Plant Immunity and Cell Death. Frontiers in Plant Science, 2022, 13, 824585.	1.7	5
4	Arabidopsis alkaline ceramidase ACER functions in defense against insect herbivory. Journal of Experimental Botany, 2022, 73, 4954-4967.	2.4	4
5	Sphingolipids in plant immunity. Phytopathology Research, 2022, 4, .	0.9	6
6	Plasma membrane-nucleo-cytoplasmic coordination of a receptor-like cytoplasmic kinase promotes EDS1-dependent plant immunity. Nature Plants, 2022, 8, 802-816.	4.7	30
7	Insights into genomic evolution from the chromosomal and mitochondrial genomes of Ustilaginoidea virens. Phytopathology Research, 2021, 3, .	0.9	9
8	The immune components ENHANCED DISEASE SUSCEPTIBILITY 1 and PHYTOALEXIN DEFICIENT 4 are required for cell death caused by overaccumulation of ceramides in Arabidopsis. Plant Journal, 2021, 107, 1447-1465.	2.8	19
9	Jasmonates modulate sphingolipid metabolism and accelerate cell death in the ceramide kinase mutant <i>acd5</i> . Plant Physiology, 2021, 187, 1713-1727.	2.3	8
10	Functions of Sphingolipids in Pathogenesis During Host–Pathogen Interactions. Frontiers in Microbiology, 2021, 12, 701041.	1.5	26
11	High-yield monolayer graphene grids for near-atomic resolution cryoelectron microscopy. Proceedings of the National Academy of Sciences of the United States of America, 2020, 117, 1009-1014.	3.3	84
12	The <i>Arabidopsis At</i> GCD3 protein is a glucosylceramidase that preferentially hydrolyzes long-acyl-chain glucosylceramides. Journal of Biological Chemistry, 2020, 295, 717-728.	1.6	7
13	Quantum-limit Chern topological magnetism in TbMn6Sn6. Nature, 2020, 583, 533-536.	13.7	253
14	Fumonisin B1: A Tool for Exploring the Multiple Functions of Sphingolipids in Plants. Frontiers in Plant Science, 2020, 11, 600458.	1.7	26
15	Fermion–boson many-body interplay in a frustrated kagome paramagnet. Nature Communications, 2020, 11, 4003.	5.8	35
16	The Arabidopsis KH-domain protein FLOWERING LOCUS Y delays flowering by upregulating FLOWERING LOCUS C family members. Plant Cell Reports, 2020, 39, 1705-1717.	2.8	3
17	Ceramide-Induced Cell Death Depends on Calcium and Caspase-Like Activity in Rice. Frontiers in Plant Science, 2020, 11, 145.	1.7	23
18	Petroleum pitch: Exploring a 50-year structure puzzle with real-space molecular imaging. Carbon, 2020, 161, 456-465.	5.4	50

#	Article	IF	CITATIONS
19	A Pyrimidin-Like Plant Activator Stimulates Plant Disease Resistance and Promotes the Synthesis of Primary Metabolites. International Journal of Molecular Sciences, 2020, 21, 2705.	1.8	1
20	The Arabidopsis AtGCD3 protein is a glucosylceramidase that preferentially hydrolyzes long-acyl-chain glucosylceramides. Journal of Biological Chemistry, 2020, 295, 717-728.	1.6	9
21	Understanding solution processing of inorganic materials using cryo-EM. Optical Materials Express, 2020, 10, 119.	1.6	3
22	Salt Enhances Disease Resistance and Suppresses Cell Death in Ceramide Kinase Mutants. Plant Physiology, 2019, 181, 319-331.	2.3	18
23	Extending the Photovoltaic Response of Perovskite Solar Cells into the Nearâ€Infrared with a Narrowâ€Bandgap Organic Semiconductor. Advanced Materials, 2019, 31, e1904494.	11.1	71
24	Soft Chemical Synthesis of H _{<i>x</i>} CrS ₂ : An Antiferromagnetic Material with Alternating Amorphous and Crystalline Layers. Journal of the American Chemical Society, 2019, 141, 15634-15640.	6.6	31
25	Emergence of membrane sphingolipids as a potential therapeutic target. Biochimie, 2019, 158, 257-264.	1.3	15
26	Humidity and Strain Rate Determine the Extent of Phase Shift in the Piezoresistive Response of PEDOT:PSS. ACS Applied Materials & Interfaces, 2019, 11, 16888-16895.	4.0	12
27	Nitrogen-plasma treated hafnium oxyhydroxide as an efficient acid-stable electrocatalyst for hydrogen evolution and oxidation reactions. Nature Communications, 2019, 10, 1543.	5.8	50
28	BIK1 and ERECTA Play Opposing Roles in Both Leaf and Inflorescence Development in Arabidopsis. Frontiers in Plant Science, 2019, 10, 1480.	1.7	7
29	Autophagy in Plant Immunity. Advances in Experimental Medicine and Biology, 2019, 1209, 23-41.	0.8	12
30	Loss of alkaline ceramidase inhibits autophagy in Arabidopsis and plays an important role during environmental stress response. Plant, Cell and Environment, 2018, 41, 837-849.	2.8	30
31	Niclosamide Blocks Rice Leaf Blight by Inhibiting Biofilm Formation of Xanthomonas oryzae. Frontiers in Plant Science, 2018, 9, 408.	1.7	38
32	Influence of Bulky Organoâ€Ammonium Halide Additive Choice on the Flexibility and Efficiency of Perovskite Lightâ€Emitting Devices. Advanced Functional Materials, 2018, 28, 1802060.	7.8	76
33	Anisotropic crystallization in solution processed chalcogenide thin film by linearly polarized laser. Applied Physics Letters, 2017, 110, .	1.5	11
34	The Arabidopsis Mitochondrial Protease FtSH4 Is Involved in Leaf Senescence via Regulation of WRKY-Dependent Salicylic Acid Accumulation and Signaling. Plant Physiology, 2017, 173, 2294-2307.	2.3	98
35	The <i>Ralstonia solanacearum</i> effector RipAK suppresses plant hypersensitive response by inhibiting the activity of host catalases. Cellular Microbiology, 2017, 19, e12736.	1.1	40
36	Electrical Stress Influences the Efficiency of CH ₃ NH ₃ PbI ₃ Perovskite Light Emitting Devices. Advanced Materials, 2017, 29, 1605317.	11.1	105

#	Article	IF	CITATIONS
37	Photoluminescence of Functionalized Germanium Nanocrystals Embedded in Arsenic Sulfide Glass. ACS Applied Materials & Interfaces, 2017, 9, 18911-18917.	4.0	10
38	PMN-PT nanostructures for energy scavenging. Semiconductor Science and Technology, 2017, 32, 063001.	1.0	4
39	Stable synthesis of few-layered boron nitride nanotubes by anodic arc discharge. Scientific Reports, 2017, 7, 3075.	1.6	50
40	<i>In Situ</i> Preparation of Metal Halide Perovskite Nanocrystal Thin Films for Improved Light-Emitting Devices. ACS Nano, 2017, 11, 3957-3964.	7.3	151
41	Mixed-Halide Perovskites with Stabilized Bandgaps. Nano Letters, 2017, 17, 6863-6869.	4.5	165
42	The promoting effect of tetravalent cerium on the oxygen evolution activity of copper oxide catalysts. Physical Chemistry Chemical Physics, 2017, 19, 31545-31552.	1.3	44
43	Extremely Low Operating Current Resistive Memory Based on Exfoliated 2D Perovskite Single Crystals for Neuromorphic Computing. ACS Nano, 2017, 11, 12247-12256.	7.3	286
44	Activity of pure and transition metal-modified CoOOH for the oxygen evolution reaction in an alkaline medium. Journal of Materials Chemistry A, 2017, 5, 842-850.	5.2	158
45	Understanding Polymorph Transformations in Coreâ€Chlorinated Naphthalene Diimides and their Impact on Thinâ€Film Transistor Performance. Advanced Functional Materials, 2016, 26, 2357-2364.	7.8	42
46	A Role of the FUZZY ONIONS LIKE Gene in Regulating Cell Death and Defense in Arabidopsis. Scientific Reports, 2016, 6, 37797.	1.6	5
47	Atomic-Scale Visualization of Quasiparticle Interference on a Type-II Weyl Semimetal Surface. Physical Review Letters, 2016, 117, 266804.	2.9	56
48	Energy scavenging based on a single-crystal PMN-PT nanobelt. Scientific Reports, 2016, 6, 22513.	1.6	24
49	Orosomucoid Proteins Interact with the Small Subunit of Serine Palmitoyltransferase and Contribute to Sphingolipid Homeostasis and Stress Responses in Arabidopsis. Plant Cell, 2016, 28, 3038-3051.	3.1	57
50	Structural variations of the cathode deposit in the carbon arc. Carbon, 2016, 105, 490-495.	5.4	27
51	In-situ synthesis and defect evolution of single-crystal piezoelectric nanoparticles. Nano Energy, 2016, 28, 195-205.	8.2	9
52	An ABC transporter, OsABCG26, is required for anther cuticle and pollen exine formation and pollen-pistil interactions in rice. Plant Science, 2016, 253, 21-30.	1.7	60
53	Fermi arc electronic structure and Chern numbers in the type-II Weyl semimetal candidate <mml:math xmlns:mml="http://www.w3.org/1998/Math/MathML"><mml:mrow><mml:msub><mml:mi>Mo</mml:mi><mr mathvariant="normal">W<mml:mrow><mml:mn>1</mml:mn><mml:mo>â^²</mml:mo><mml:mi>x< Physical Review B. 2016. 94</mml:mi></mml:mrow></mr </mml:msub></mml:mrow></mml:math 	nl:mişx<	nl:mi>:/mml:mrow>
54	Nanoscale electrical properties of epitaxial Cu3Ge film. Scientific Reports, 2016, 6, 28818.	1.6	8

#	Article	IF	CITATIONS
55	Nanomedicine as a non-invasive strategy for drug delivery across the blood brain barrier. International Journal of Pharmaceutics, 2016, 515, 331-342.	2.6	65
56	Dynamic nano-triboelectrification using torsional resonance mode atomic force microscopy. Scientific Reports, 2016, 6, 27874.	1.6	9
57	Atomic-Scale Visualization of Quantum Interference on a Weyl Semimetal Surface by Scanning Tunneling Microscopy. ACS Nano, 2016, 10, 1378-1385.	7.3	112
58	Laser ablation of germanium in arsenic sulfide solution. , 2016, , .		0
59	Arabidopsis acylâ€ <scp>C</scp> o <scp>A</scp> â€binding protein <scp>ACBP</scp> 3 participates in plant response to hypoxia by modulating veryâ€longâ€chain fatty acid metabolism. Plant Journal, 2015, 81, 53-67.	2.8	84
60	Surface modifications with Lissajous trajectories using atomic force microscopy. Applied Physics Letters, 2015, 107, 113102.	1.5	2
61	Single‣tep Assembly of Multimodal Imaging Nanocarriers: MRI and Longâ€Wavelength Fluorescence Imaging. Advanced Healthcare Materials, 2015, 4, 1376-1385.	3.9	48
62	A Novel Pyrimidin-Like Plant Activator Stimulates Plant Disease Resistance and Promotes Growth. PLoS ONE, 2015, 10, e0123227.	1.1	14
63	An Arabidopsis neutral ceramidase mutant ncer1 accumulates hydroxyceramides and is sensitive to oxidative stress. Frontiers in Plant Science, 2015, 6, 460.	1.7	33
64	Ethylene Modulates Sphingolipid Synthesis in Arabidopsis. Frontiers in Plant Science, 2015, 6, 1122.	1.7	27
65	Toxicity of Nanomaterials to Plants. , 2015, , 101-123.		9
66	Decagonite, Al ₇₁ Ni ₂₄ Fe ₅ , a quasicrystal with decagonal symmetry from the Khatyrka CV3 carbonaceous chondrite. American Mineralogist, 2015, 100, 2340-2343.	0.9	61
67	The Arabidopsis ceramidase <i>At</i> <scp>ACER</scp> functions in disease resistance and salt tolerance. Plant Journal, 2015, 81, 767-780.	2.8	79
68	Cu(II) Galvanic Reduction and Deposition onto Iron Nano- and Microparticles: Resulting Morphologies and Growth Mechanisms. Langmuir, 2015, 31, 789-798.	1.6	12
69	Disruption of the Arabidopsis Defense Regulator Genes SAG101, EDS1, and PAD4 Confers Enhanced Freezing Tolerance. Molecular Plant, 2015, 8, 1536-1549.	3.9	55
70	Unsaturation of Very-Long-Chain Ceramides Protects Plant from Hypoxia-Induced Damages by Modulating Ethylene Signaling in Arabidopsis. PLoS Genetics, 2015, 11, e1005143.	1.5	86
71	A systematic simulation of the effect of salicylic acid on sphingolipid metabolism. Frontiers in Plant Science, 2015, 6, 186.	1.7	17
72	A Gene Expression Profiling of Early Rice Stamen Development that Reveals Inhibition of Photosynthetic Genes by OsMADS58. Molecular Plant, 2015, 8, 1069-1089.	3.9	29

#	Article	IF	CITATIONS
73	Mechanical and hyperthermic properties of magnetic nanocomposites for biomedical applications. Journal of the Mechanical Behavior of Biomedical Materials, 2015, 49, 118-128.	1.5	10
74	Natural quasicrystal with decagonal symmetry. Scientific Reports, 2015, 5, 9111.	1.6	81
75	Bi2S3 nanowire networks as electron acceptor layers in solution-processed hybrid solar cells. Journal of Materials Chemistry C, 2015, 3, 2686-2692.	2.7	53
76	Advances in windowed gas cells for in-situ TEM studies. Nano Energy, 2015, 13, 735-756.	8.2	51
77	The (0001) surfaces of α-Fe ₂ O ₃ nanocrystals are preferentially activated for water oxidation by Ni doping. Physical Chemistry Chemical Physics, 2015, 17, 26797-26803.	1.3	8
78	Advances in sealed liquid cells for in-situ TEM electrochemial investigation of lithium-ion battery. Nano Energy, 2015, 11, 196-210.	8.2	75
79	Fabrication of uniformly dispersed nanoparticle-doped chalcogenide glass. Applied Physics Letters, 2014, 105, 261906.	1.5	14
80	MOCVD synthesis of compositionally tuned topological insulator nanowires. Physica Status Solidi - Rapid Research Letters, 2014, 8, 991-996.	1.2	13
81	Steinhardtite, a new body-centered-cubic allotropic form of aluminum from the Khatyrka CV3 carbonaceous chondrite. American Mineralogist, 2014, 99, 2433-2436.	0.9	37
82	Specific adaptation of Ustilaginoidea virens in occupying host florets revealed by comparative and functional genomics. Nature Communications, 2014, 5, 3849.	5.8	202
83	Au@carbon yolk–shell nanostructures via one-step core–shell–shell template. Chemical Communications, 2014, 50, 478-480.	2.2	116
84	One-pot Stöber route yields template for Ag@carbon yolk–shell nanostructures. Chemical Communications, 2014, 50, 9056.	2.2	51
85	Wireless biomechanical power harvesting via flexible magnetostrictive ribbons. Energy and Environmental Science, 2014, 7, 2243.	15.6	7
86	A one-step and scalable production route to metal nanocatalyst supported polymer nanospheres via flash nanoprecipitation. Journal of Materials Chemistry A, 2014, 2, 17286-17290.	5.2	30
87	Loss of Ceramide Kinase in <i>Arabidopsis</i> Impairs Defenses and Promotes Ceramide Accumulation and Mitochondrial H ₂ O ₂ Bursts. Plant Cell, 2014, 26, 3449-3467.	3.1	92
88	Impact-induced shock and the formation of natural quasicrystals in the early solar system. Nature Communications, 2014, 5, 4040.	5.8	71
89	Material Study of High Performance Single Crystal Ferroelectric Nanowires. Microscopy and Microanalysis, 2014, 20, 1968-1969.	0.2	0
90	Function and Interaction of the Coupled Genes Responsible for Pik-h Encoded Rice Blast Resistance. PLoS ONE, 2014, 9, e98067.	1.1	88

#	Article	IF	CITATIONS
91	Flexible Piezoelectric PMN–PT Nanowire-Based Nanocomposite and Device. Nano Letters, 2013, 13, 2393-2398.	4.5	290
92	Biotemplated Synthesis of PZT Nanowires. Nano Letters, 2013, 13, 6197-6202.	4.5	35
93	AtMMS21, an SMC5/6 Complex Subunit, Is Involved in Stem Cell Niche Maintenance and DNA Damage Responses in Arabidopsis Roots Â. Plant Physiology, 2013, 161, 1755-1768.	2.3	60
94	A detrimental mitochondrial-nuclear interaction causes cytoplasmic male sterility in rice. Nature Genetics, 2013, 45, 573-577.	9.4	415
95	Identification of Arabidopsis accession with resistance to Botrytis cinerea by natural variation analysis, and characterization of the resistance response. Plant Biotechnology, 2013, 30, 89-95.	0.5	4
96	Dynamics of Defense Responses and Cell Fate Change during Arabidopsis-Pseudomonas syringae Interactions. PLoS ONE, 2013, 8, e83219.	1.1	29
97	Comparative Analysis of the Genomes of Two Field Isolates of the Rice Blast Fungus Magnaporthe oryzae. PLoS Genetics, 2012, 8, e1002869.	1.5	167
98	Evidence for the extraterrestrial origin of a natural quasicrystal. Proceedings of the National Academy of Sciences of the United States of America, 2012, 109, 1396-1401.	3.3	94
99	Cellular Tolerance, Accumulation and Distribution of Cadmium in Leaves of Hyperaccumulator Picris divaricata. Pedosphere, 2012, 22, 497-507.	2.1	22
100	Programmed cell death of secretory cavity cells in fruits of Citrus grandis cv. Tomentosa is associated with activation of caspase 3-like protease. Trees - Structure and Function, 2012, 26, 1821-1835.	0.9	20
101	Effect of surface defects on InGaAs/InAlAs Quantum Cascade mesa current–voltage characteristics. Journal of Crystal Growth, 2012, 353, 35-38.	0.7	1
102	Fabrication and piezoelectric property of PMN-PT nanofibers. Nano Energy, 2012, 1, 602-607.	8.2	36
103	In Situ Mechanical and Electrical Characterization of Individual <scp>TiO</scp> ₂ Nanofibers Using a Nanomanipulator System. Scanning, 2012, 34, 341-346.	0.7	5
104	Ultrastable nanostructured polymer glasses. Nature Materials, 2012, 11, 337-343.	13.3	150
105	PMN-PT Nanowires with a Very High Piezoelectric Constant. Nano Letters, 2012, 12, 2238-2242.	4.5	76
106	Young's Modulus Determination of Unpolled Electrospun PZT Nanofibers. Science of Advanced Materials, 2012, 4, 847-850.	0.1	2
107	Growth of Straight Silicon Nanowires on Amorphous Substrates with Uniform Diameter, Length, Orientation, and Location Using Nanopatterned Host-Mediated Catalyst. Nano Letters, 2011, 11, 5247-5251.	4.5	16
108	Rutherford backscattering oscillation in scanning helium-ion microscopy. Journal of Applied Physics, 2011, 109, 064311.	1.1	9

#	Article	IF	CITATIONS
109	Energy Harvesting Based on PZT Nanofibers. Green Energy and Technology, 2011, , 425-438.	0.4	8
110	Icosahedrite, Al63Cu24Fe13, the first natural quasicrystal. American Mineralogist, 2011, 96, 928-931.	0.9	165
111	Ligand Effects and Synthesis of NaYF ₄ Based Up and Downconversion Colloidal Nanophosphors. ACS Symposium Series, 2011, , 71-85.	0.5	2
112	A Conserved Cysteine Motif Is Critical for Rice Ceramide Kinase Activity and Function. PLoS ONE, 2011, 6, e18079.	1.1	20
113	Pegylated Composite Nanoparticles Containing Upconverting Phosphors and <i>meso</i> â€Tetraphenyl porphine (TPP) for Photodynamic Therapy. Advanced Functional Materials, 2011, 21, 2488-2495.	7.8	172
114	A wire microcalorimetric study of catalytic ignition of methane–air mixtures over palladium oxide. Proceedings of the Combustion Institute, 2011, 33, 1819-1825.	2.4	7
115	Adjustable stiffness of individual piezoelectric nanofibers by electron beam polarization. Applied Physics Letters, 2011, 99, .	1.5	8
116	Synthesis of Stable Block-Copolymer-Protected NaYF ₄ :Yb ³⁺ , Er ³⁺ Up-Converting Phosphor Nanoparticles. Chemistry of Materials, 2010, 22, 311-318.	3.2	137
117	Phase transition induced formation of hollow structures in colloidal lanthanide-doped NaYF4 nanocrystals. Journal of Nanoparticle Research, 2010, 12, 1429-1438.	0.8	21
118	Anomalous Raman Scattering of Colloidal Yb ³⁺ ,Er ³⁺ Codoped NaYF ₄ Nanophosphors and Dynamic Probing of the Upconversion Luminescence. Advanced Functional Materials, 2010, 20, 3530-3537.	7.8	91
119	Effect of the hfq gene on 2,4-diacetylphloroglucinol production and the Pcol/PcoR quorum-sensing system in Pseudomonas fluorescens 2P24. FEMS Microbiology Letters, 2010, 309, no-no.	0.7	32
120	Possible animal-body fossils in pre-Marinoan limestones from South Australia. Nature Geoscience, 2010, 3, 653-659.	5.4	180
121	Adhesion and the cold welding of gold-silver thin films. Journal of Applied Physics, 2010, 107, 043519.	1.1	30
122	An investigation of the thermal sensitivity and stability of the β-NaYF4:Yb,Er upconversion nanophosphors. Journal of Applied Physics, 2010, 107, 054901.	1.1	62
123	Ultralow Superharmonic Resonance for Functional Nanowires. Nano Letters, 2010, 10, 852-859.	4.5	19
124	The Hidden Effects of Particle Shape and Criteria for Evaluating the Upconversion Luminescence of the Lanthanide Doped Nanophosphors. Journal of Physical Chemistry C, 2010, 114, 2452-2461.	1.5	103
125	1.6 V Nanogenerator for Mechanical Energy Harvesting Using PZT Nanofibers. Nano Letters, 2010, 10, 2133-2137.	4.5	808
126	Induction of programmed cell death in <i>Arabidopsis</i> and rice by singleâ€wall carbon nanotubes. American Journal of Botany, 2010, 97, 1602-1609.	0.8	218

#	Article	IF	CITATIONS
127	Natural Quasicrystals. Science, 2009, 324, 1306-1309.	6.0	243
128	Potential measurement from a single lead ziroconate titanate nanofiber using a nanomanipulator. Applied Physics Letters, 2009, 94, .	1.5	80
129	Organic–inorganic interfaces and spiral growth in nacre. Journal of the Royal Society Interface, 2009, 6, 367-376.	1.5	50
130	Stabilizing cyanosols: amorphous cyanide bridged transition metal polymer nanoparticles. Journal of Materials Chemistry, 2009, 19, 8846.	6.7	8
131	Superior imaging resolution in scanning helium-ion microscopy: A look at beam-sample interactions. Journal of Applied Physics, 2008, 104, .	1.1	61
132	A J Domain Virulence Effector of Pseudomonas syringae Remodels Host Chloroplasts and Suppresses Defenses. Current Biology, 2007, 17, 499-508.	1.8	266
133	Europium-doped yttrium silicate nanophosphors prepared by flame synthesis. Materials Research Bulletin, 2007, 42, 1440-1449.	2.7	48
134	Induction of Apoptotic Cell Death Leads to the Development of Bacterial Rot Caused by Pseudomonas cichorii. Molecular Plant-Microbe Interactions, 2006, 19, 112-122.	1.4	27
135	Arabidopsis ACCELERATED CELL DEATH2 Modulates Programmed Cell Death. Plant Cell, 2006, 18, 397-411.	3.1	221
136	The role and regulation of programmed cell death in plant-pathogen interactions. Cellular Microbiology, 2004, 6, 201-211.	1.1	649
137	The mitochondrion - an organelle commonly involved in programmed cell death in Arabidopsis thaliana. Plant Journal, 2004, 40, 596-610.	2.8	253
138	Nitric Oxide and Reactive Oxygen Species Do Not Elicit Hypersensitive Cell Death but Induce Apoptosis in the Adjacent Cells During the Defense Response of Oat. Molecular Plant-Microbe Interactions, 2004, 17, 245-253.	1.4	102
139	Ceramides modulate programmed cell death in plants. Genes and Development, 2003, 17, 2636-2641.	2.7	321
140	Apoptotic Cell Death is a Common Response to Pathogen Attack in Oats. Molecular Plant-Microbe Interactions, 2002, 15, 1000-1007.	1.4	59
141	Mitochondrial oxidative burst involved in apoptotic response in oats. Plant Journal, 2002, 30, 567-579.	2.8	131
142	Novel evidence for apoptotic cell response and differential signals in chromatin condensation and DNA cleavage in victorin-treated oats. Plant Journal, 2001, 28, 13-26.	2.8	83
143	Molecular mechanics of binding in carbon-nanotube–polymer composites. Journal of Materials Research, 2000, 15, 2770-2779.	1.2	334
144	Nanocomposite Mullite/Mullite Powders by Spray Pyrolysis. Journal of Nanoparticle Research, 1999, 1, 127-130.	0.8	9

#	Article	IF	CITATIONS
145	Synthesis of Photonic Crystals for Optical Wavelengths from Semiconductor Quantum Dots. Advanced Materials, 1999, 11, 165-169.	11.1	355
146	Layer by layer imaging of diblock copolymer films with a scanning electron microscope. Polymer, 1998, 39, 2733-2744.	1.8	81
147	Young's modulus of single-walled carbon nanotubes. Journal of Applied Physics, 1998, 84, 1939-1943.	1.1	344
148	Biomimetic Synthesis of Macroscopic-Scale Calcium Carbonate Thin Films. Evidence for a Multistep Assembly Process. Journal of the American Chemical Society, 1998, 120, 11977-11985.	6.6	277
149	Depth Profiling Block Copolymer Microdomains. Macromolecules, 1998, 31, 2185-2189.	2.2	100
150	Radial compression and controlled cutting of carbon nanotubes. Journal of Chemical Physics, 1998, 109, 2509-2512.	1.2	60
151	Carbon nanotube caps as springs: Molecular dynamics simulations. Physical Review B, 1998, 58, 12649-12651.	1.1	29
152	Porphyrin Amphiphiles as Templates for the Nucleation of Calcium Carbonate. Journal of the American Chemical Society, 1997, 119, 5449-5450.	6.6	82
153	Nanoscale Patterning of Barium Titanate on Block Copolymers. Langmuir, 1997, 13, 3866-3870.	1.6	34
154	Biomimetic fabrication of materials: the minimalist approach. , 1996, 2716, 317.		1
155	Convergent Beam Electron Diffraction and High Resolution Electron Microscopy of CaFeTi2O6Perovskite. Journal of Solid State Chemistry, 1996, 123, 73-82.	1.4	8
156	Transmission electron diffraction of the ordering transformation in crystallineC60. Physical Review B, 1992, 45, 11366-11369.	1.1	22
157	Observation of double line contrast in surface imaging. Microscopy Research and Technique, 1992, 20, 413-425.	1.2	8
158	Electron diffraction conditions and surface imaging in reflection electron microscopy. Ultramicroscopy, 1990, 33, 237-254.	0.8	16
159	The parabolas and circles in RHEED patterns. Ultramicroscopy, 1989, 31, 149-157.	0.8	15
160	REM and REELS identifications of atomic terminations at α-alumina (01̄1) surface. Surface Science, 1989, 208, 533-549.	0.8	29
161	The observation of surface resonance effects in RHEED patterns. Ultramicroscopy, 1988, 26, 189-194.	0.8	26

162 Applications for biological materials. , 0, , 337-354.